

Intravital molecular imaging reveals that ROS-caspase-3-GSDME-induced cell punching enhances humoral immunotherapy targeting intracellular tumor antigens

Bolei Dai,^{1†} Ren Zhang,^{1†} Shuhong Qi,^{1*} Lei Liu,¹ Xian Zhang,¹ Deqiang Deng,¹
Jie Zhang,¹ Yilun Xu,² Fanxuan Liu,¹ Zheng Liu,¹ Qingming Luo,² and Zhihong
Zhang^{1,2*}

¹Britton Chance Center and MoE Key Laboratory for Biomedical Photonics, Wuhan National Laboratory for Optoelectronics-Huazhong University of Science and Technology, Wuhan, Hubei 430074, China

²School of Biomedical Engineering, Hainan University, Haikou, Hainan 570228, China

† These authors contributed equally to this work

* Correspondence: Zhihong Zhang, czyzzh@mail.hust.edu.cn;
Shuhong Qi, qishuhong@hust.edu.cn;

Address: Room G304, Britton Chance Center for Biomedical Photonics, Wuhan National Laboratory for Optoelectronics-Huazhong University of Science and Technology, Wuhan, Hubei 430074, China

Fax: +86-27-87792034; Tel: +86-27-87792033;

Zhihong Zhang (czyzzh@mail.hust.edu.cn) and Shuhong Qi (qishuhong@hust.edu.cn) are the corresponding authors for communication with the Editorial and Production offices.

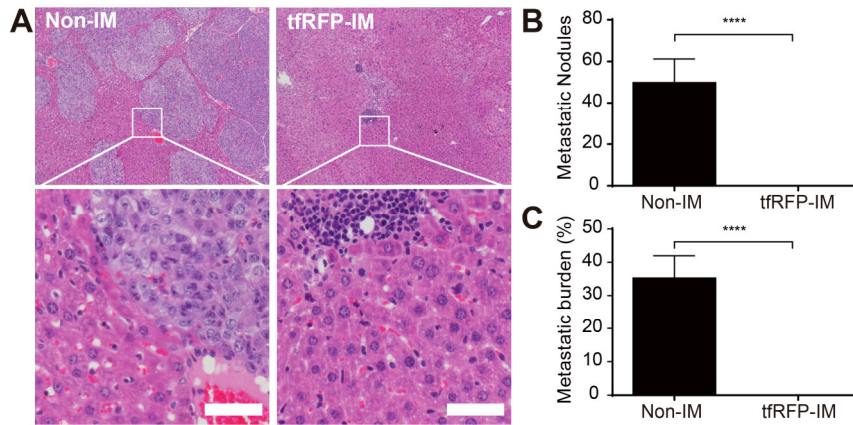


Figure S1. Hematoxylin and Eosin (HE) staining of livers from tfRFP-immunized and non-immunized mice. (A) A representative image of liver HE staining in tfRFP-immunized and non-immunized groups. Scale bar in the large image, 300 µm. Scale bar in the enlarged image, 50 µm. (B and C) Quantification of metastatic nodules and metastatic burden in (A). Data from 5 livers; each had five lobes. Data are presented as mean ± SEM. Statistical analysis was performed using the Mann Whitney test, **** $P < 0.0001$.

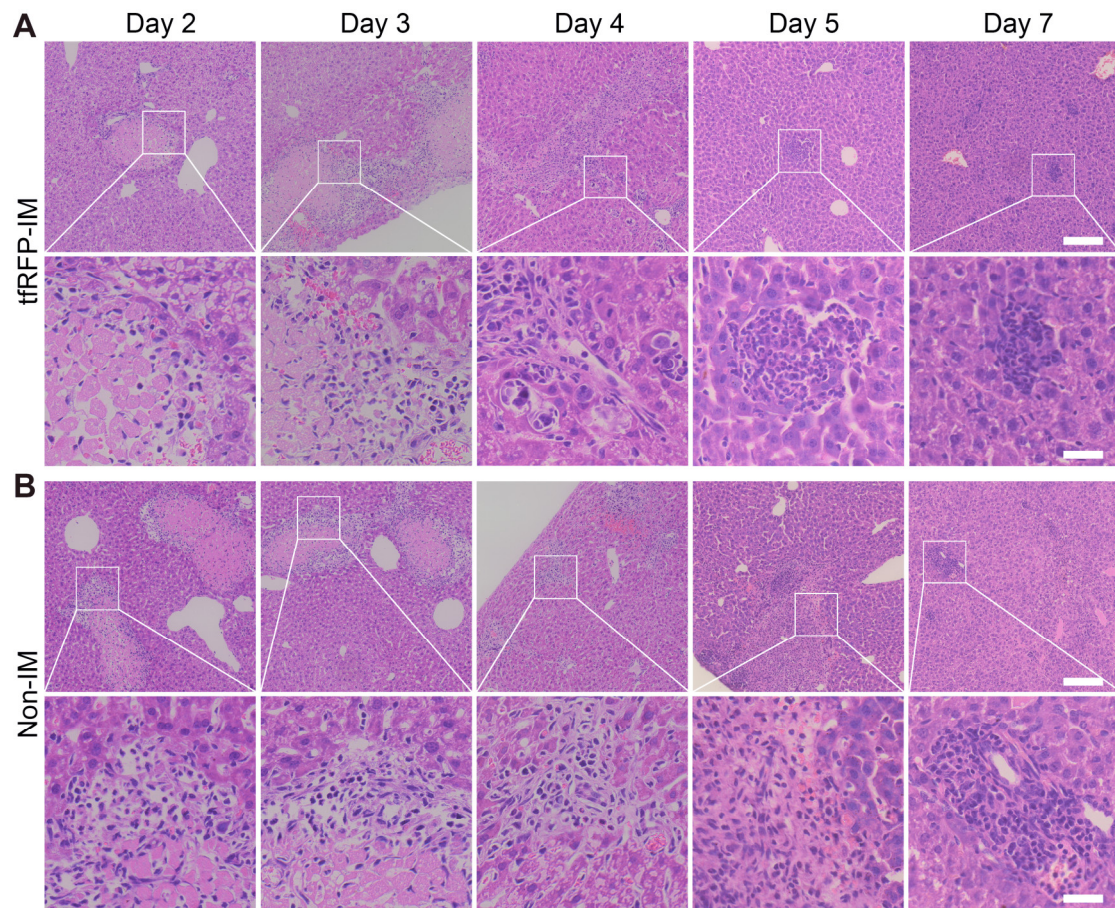


Figure S2. Representative HE staining sections of livers on Day 2/3/4/5/7 after tfRFP-B16 tumor cells injection. The images are from (A) tfRFP-immunized mice and (B) non-immunized mice. The up rows are large images, Scale bar, 150 μm . The bottom rows are enlarged images, Scale bar, 30 μm .

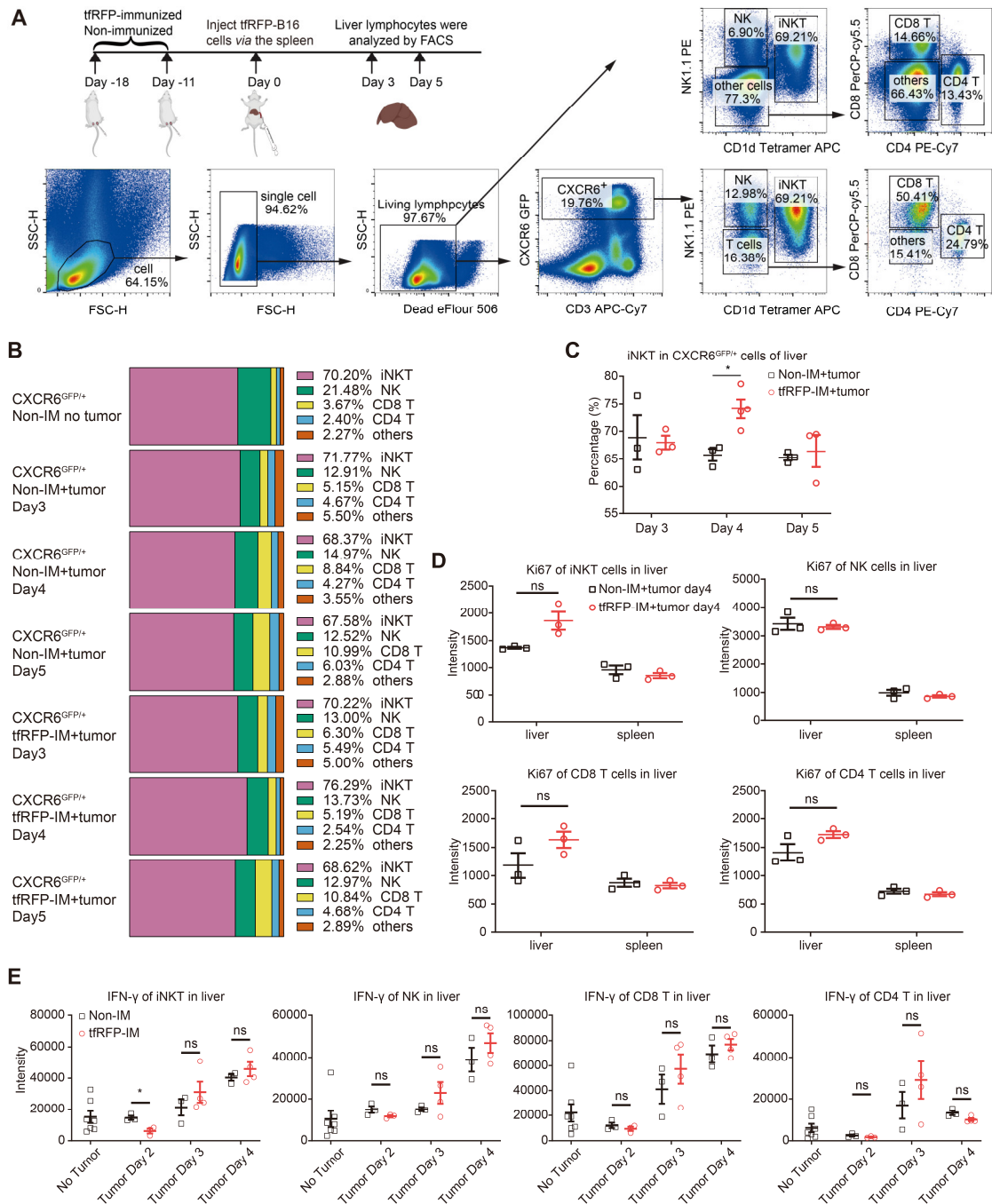


Figure S3. Flow cytometry analysis of hepatic lymphocytes of livers at different days after tumor cells incubation. (A) Schedules for liver lymphocytes FACS analysis after liver metastases and flow cytometry logic gates. **(B)** The composition ratio of lymphocytes in the hepatic CXCR6-GFP cells of tFRFP-immunized and non-immunized mice after tFRFP-B16 cell inoculation on different days ($n = 3$ per group). CXCR6^{GFP/+} Non-IM mice without tumor served as normal control group. **(C)** The proportion of iNKT cells in CXCR6-GFP cells on different inoculation days in tFRFP-immunized and non-immunized mice. Each data point represents data from a mouse. Data are presented as mean \pm SEM. Statistical analysis was performed using the unpaired Student's t -

test, $*P < 0.05$. **(D)** Ki67 expression of lymphocytes in the liver of tRFp-immunized and non-immunized mice on day 4 after tRFp-B16 injection. Each data point represents data from a mouse. Data are presented as mean \pm SEM. Statistical analysis was performed using the Mann Whitney test, ns: not significant. **(E)** IFN- γ expression of lymphocytes in the liver of tRFp-immunized and non-immunized mice on day 4 after tRFp-B16 injection. Data are presented as mean \pm SEM. Statistical analysis was performed using the Mann Whitney test, ns: not significant, $*P < 0.05$.

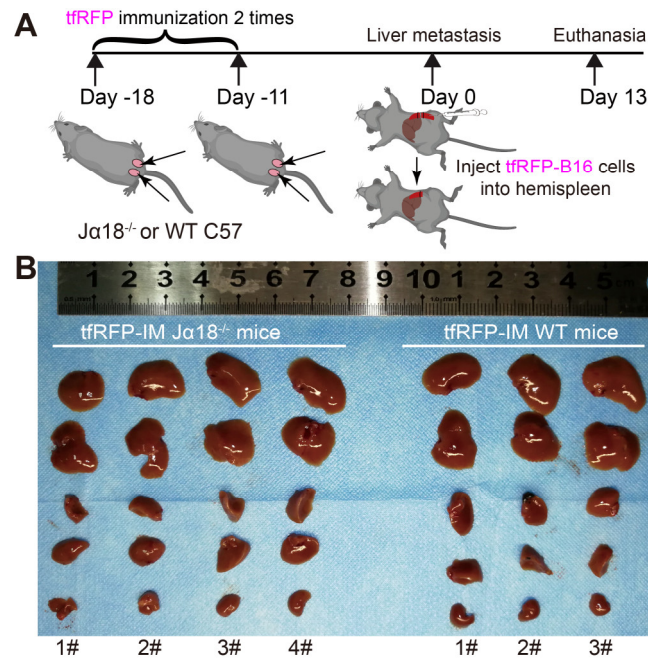


Figure S4. iNKT cell deficiency did not affect the clearing of tfRFP-B16 by the tfRFP-elicited immune response. (A) Schedules for the liver metastasis model in iNKT cell-deficient mice ($J\alpha 18^{-/-}$) or wild-type mice (WT) after tfRFP-immunization. (B) Representative white-light imaging of the 5 lobes of livers from iNKT cell-deficient mice ($J\alpha 18^{-/-}$) or wild-type mice (WT) after tfRFP-immunization.

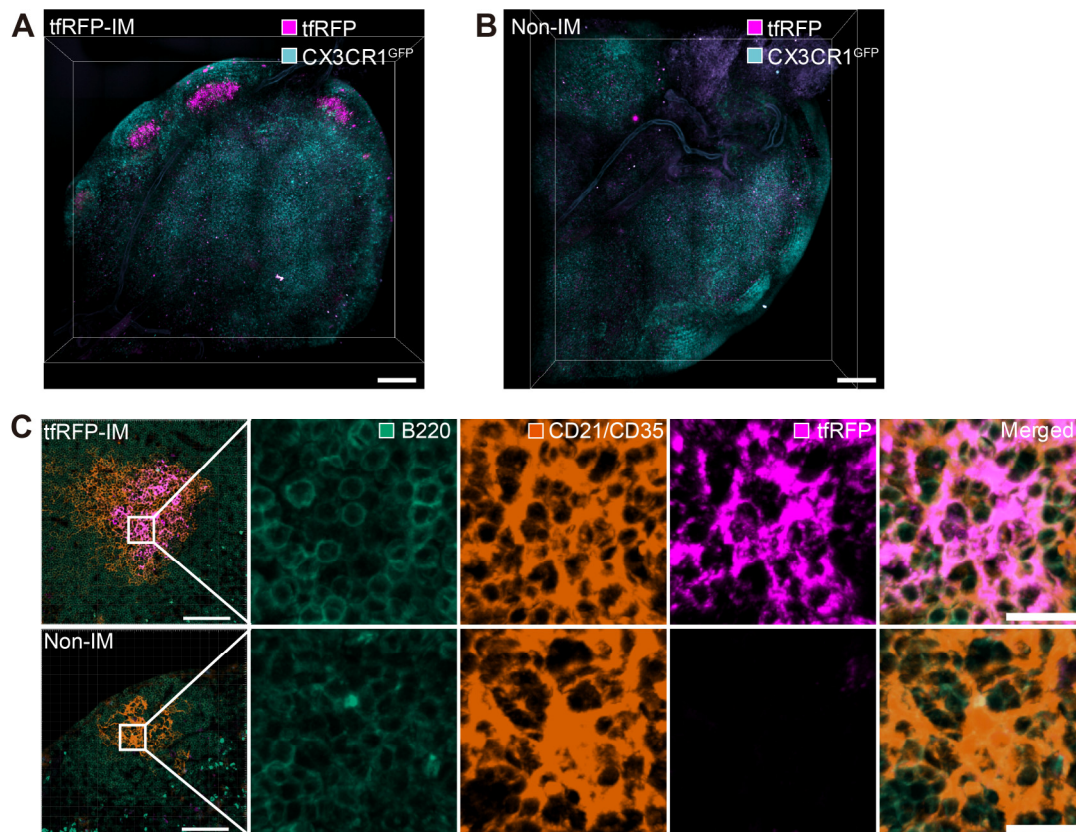


Figure S5. tFRFP is stored in fDCs in the germinal centers of inguinal lymph nodes. (A and B) Representative 3D images of inguinal lymph nodes from mice 18 days after the first immunization; (A) is the tFRFP-immunized group, and (B) is the non-immunized group. Scale bar, 300 μm . (C) Representative immunofluorescence images of inguinal lymph nodes in tFRFP-immunized mice (top row) and the non-immunized mice (bottom row). Scale bar of large field images, 50 μm . Scale bar of enlarged images, 10 μm .

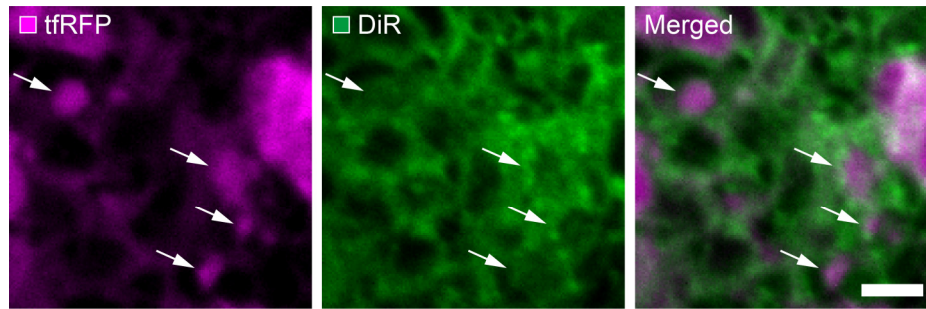


Figure S6. tfRFP⁺ particles in the liver of non-immunized mice have a membrane structure.

Representative tissue fluorescence confocal images of the tfRFP-B16 cells forming tfRFP⁺ particles, which were stained with DiR (a membrane dye). The white arrow indicates DiR positive tfRFP⁺ particles in the non-immunized group. Scale bar, 10 μ m.

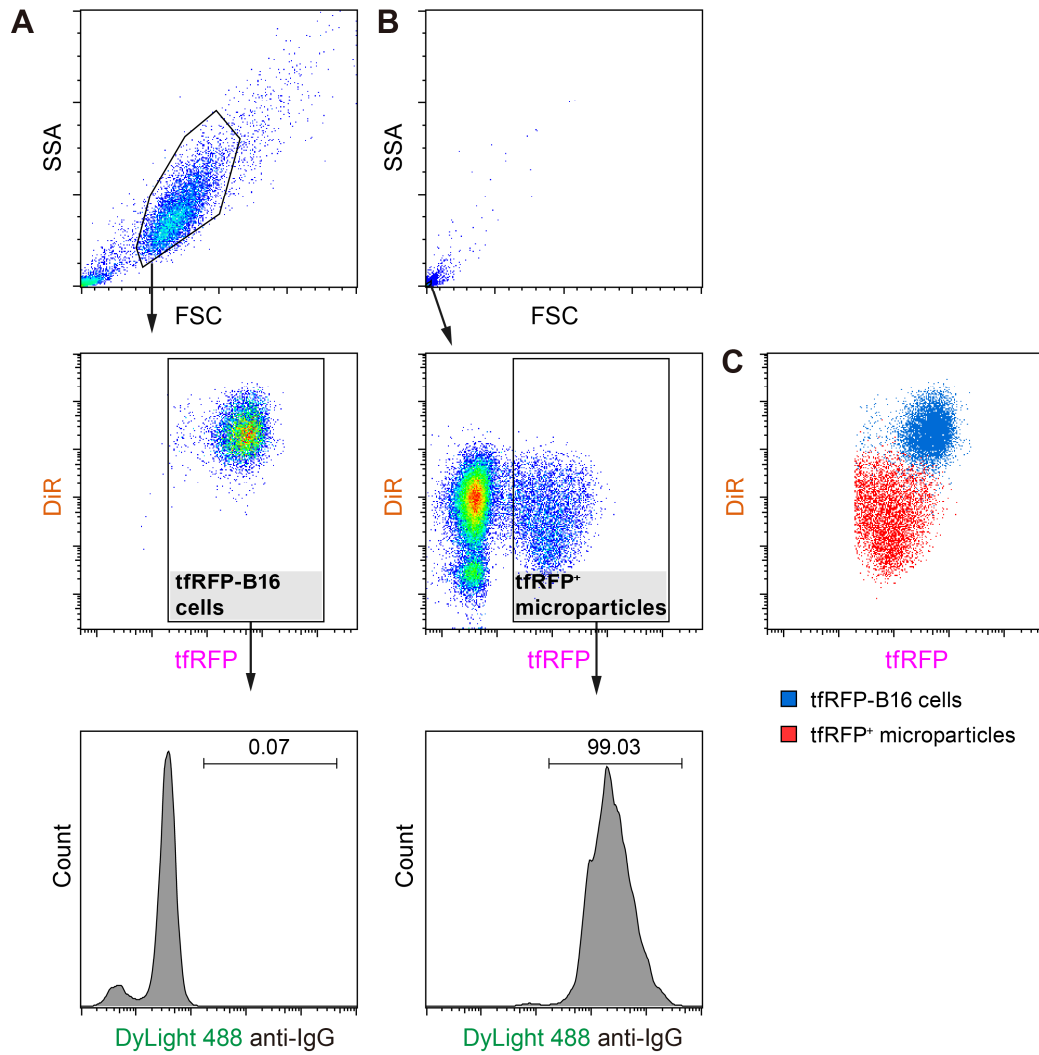


Figure S7. Flow cytometry verified tFRFP⁺ microparticles were antigen-antibody complexes.

(A) Flow cytometry results of untreated tFRFP-B16 cells labeled with DyLight 488 anti-IgG and the membrane dye DiR. (B) Flow cytometry results of tFRFP⁺ microparticles (from supernatant of tFRFP-B16 cells treated with melittin and anti-tFRFP IgG) labeled with DyLight 488 anti-IgG and the membrane dye DiR. (C) Flow scatter plot of a mixture of tFRFP⁺ microparticles and tFRFP-B16 cells. tFRFP-B16 cells were in blue and tFRFP⁺ microparticles were in red.

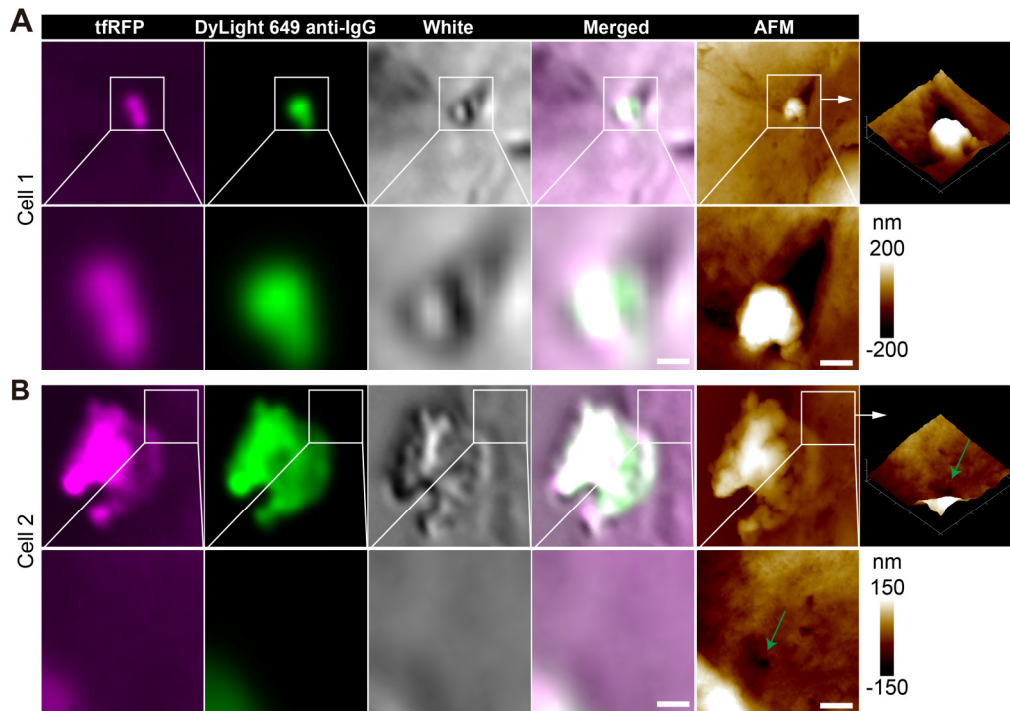


Figure S8. Representative confocal images and AFM images of the same cells stained with the DyLight 649 anti-mouse IgG antibody. (A) Representative immunofluorescence confocal imaging and AFM imaging of two tfRFP-B16 cells stained with the DyLight 649 anti-mouse IgG antibody after treatment with tfRFP-immunized serum for 4 hours. Scale bar, 1 μm . (B) Representative immunofluorescence confocal imaging and AFM imaging of two tfRFP-B16 cells stained with the DyLight 649 anti-mouse IgG antibody after treatment with tfRFP-immunized serum for 4 hours. The green arrow in the AFM image points to the hole near the tfRFP⁺ microparticle. Scale bar, 1 μm .

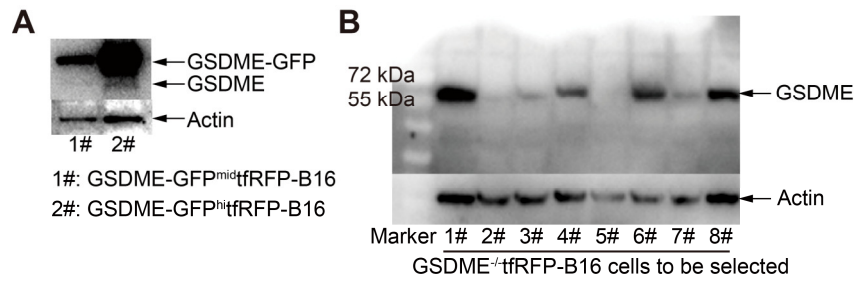


Figure S9. Identification of GSDME expression in GSDME-GFP^{mid}tfRFP-B16, GSDME-GFP^{hi}tfRFP-B16 and GSDME^{-/-}tfRFP-B16 cells. (A) Western blot analysis of GSDME-GFP^{mid}tfRFP-B16 cells and GSDME-GFP^{hi}tfRFP-B16 cells. (B) Western blot analysis of candidate GSDME^{-/-}tfRFP-B16 cells. β -Actin was used as the loading control in both cell groups.

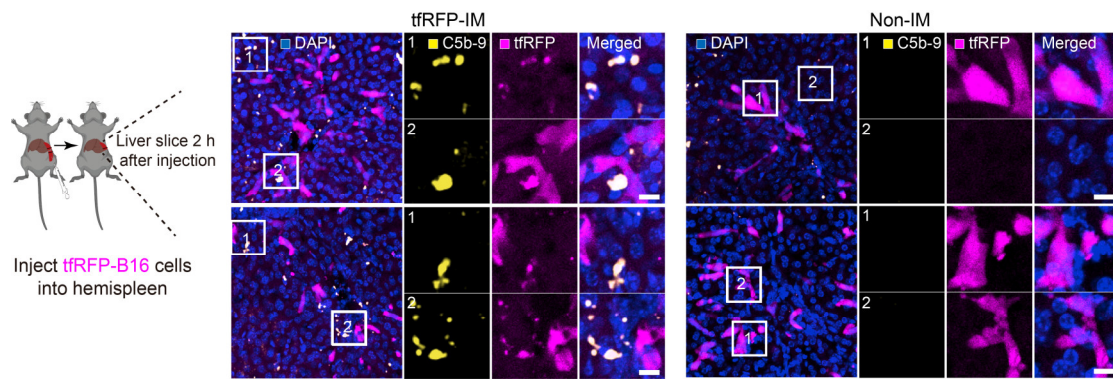


Figure S10. Complement membrane attack complex formed on tfRFP-B16 cells in the tfRFP-immunized group. Representative immunofluorescence images of C5b-9 in the liver 2 hours after tumor cell injection. Scale bar, 10 μ m.

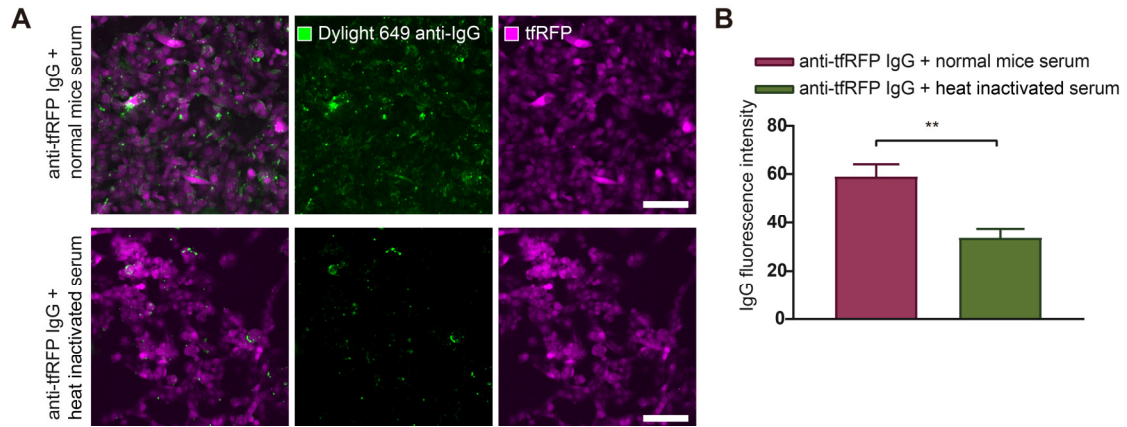


Figure S11. The complement system enhanced anti-tfRFP IgG binding to the cell membranes.

(A) Representative confocal images of cultured tfRFP-B16 cells after 4 hours of incubation with anti-tfRFP IgG plus normal mouse serum or anti-tfRFP IgG plus heat-inactivated mouse serum. (B)

Statistics of the fluorescence intensity of the IgG channel in (A). Data are presented as mean ± SEM.

Statistical analysis was performed using unpaired Student's *t*-test, ** $P < 0.01$.

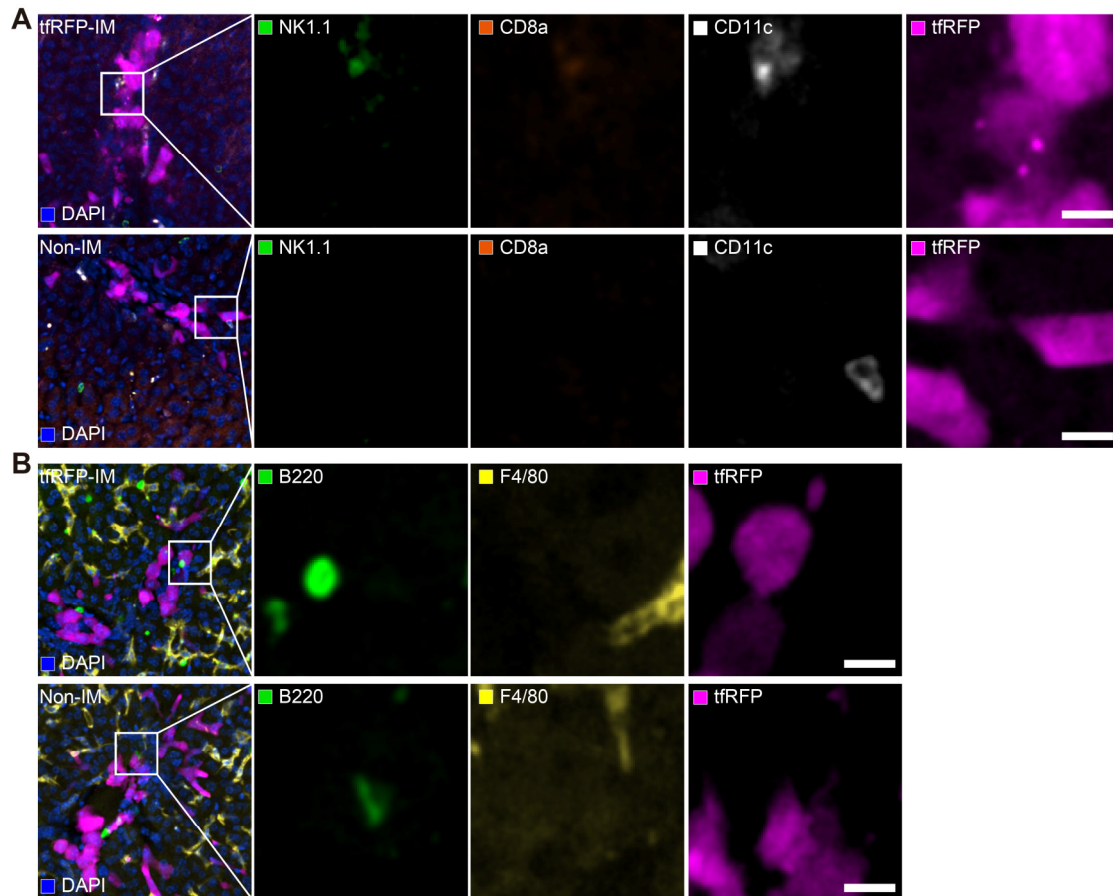


Figure S12. NK cells, CD8⁺ T cells, B cells, DCs, and macrophages were not recruited in the early stage. (A) Representative images of NK cells (NK1.1⁺), CD8⁺ T cells (CD8a⁺) and DCs (CD11c⁺) near the tfRFP-B16 tumor cells 2 hours after tfRFP-B16 cells injection. Scale bar, 10 μm. (B) Representative images of B cells (B220⁺), and macrophages (F4/80⁺) near the tfRFP-B16 tumor cells 2 hours after tfRFP-B16 cells injection. Scale bar, 10 μm.

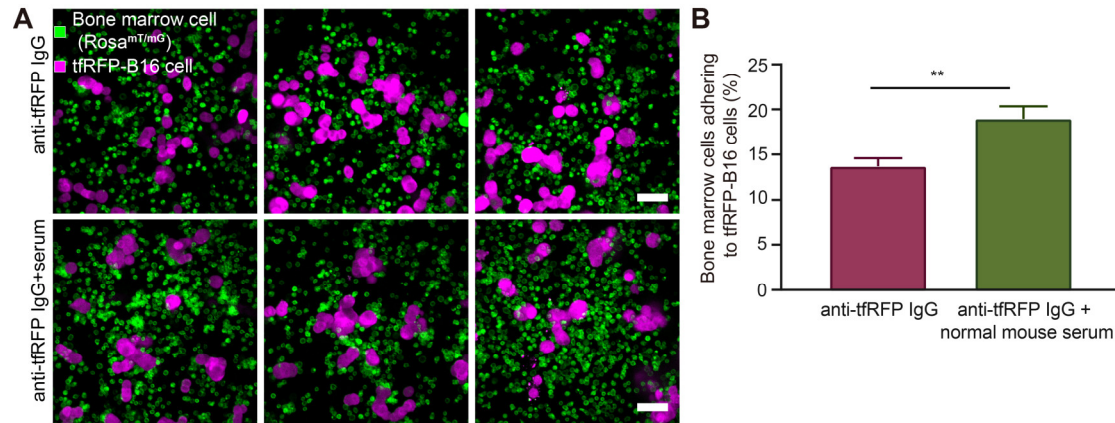


Figure S13. *In vitro* cell experiment of neutrophils recruitment. (A) Representative live cell confocal images of tfRFP-B16 cells co-cultured with bone marrow cells (about 60% of them were neutrophils) from ROSA^{mT/mG} mice were treated with anti-tfRFP IgG plus normal mouse serum or anti-tfRFP IgG alone for 2 hours. Scale bar, 50 μ m. (B) Statistics of the proportion of bone marrow cells contacted with tfRFP-B16 cells in all bone marrow cells. Data are presented as mean \pm SEM. Statistical analysis was performed using the unpaired Student's *t* test, **P* < 0.05.



Figure S14. Macrophages surround cleared liver metastasis. F4/80⁺ macrophages formed a circle at the site of tfRFP-B16 cell clearance in livers of tfRFP-immunized mice on day 5 after tfRFP-B16 cells injection. Scale bar, 100 μ m.

Movie S1: *In vivo* time-lapse imaging of the infiltrated CXCR6-GFP cells and tRFFP⁺ microparticles in tRFFP-B16 metastasis of liver in tRFFP-immunized mice on Day 3. Time-lapse intravital imaging was acquired by oil 60×/1.42 NA objective. CXCR6-GFP cells are shown in green, and tRFFP-B16 cells and tRFFP⁺ microparticles are shown in magenta. Scale bar, 20 μm.

Movie S2: *In vivo* time-lapse imaging of the disruption of tRFFP-B16 cells to form tRFFP⁺ microparticles within the first hour of tRFFP-B16 inoculation in the tRFFP-immunized mice. Time-lapse intravital imaging was acquired by air 20×/0.75 NA objective. tRFFP-B16 cells and tRFFP⁺ microparticles are shown in magenta. Scale bar, 30 μm.

Movie S3: *In vivo* time-lapse imaging of the formation of tRFFP⁺ particles within the first hour of tRFFP-B16 inoculation in the non-immunized mice. Time-lapse intravital imaging was acquired by air 20×/0.75 NA objective. tRFFP-B16 cells and tRFFP⁺ particles are shown in magenta. Scale bar, 30 μm.

Movie S4: *In vivo* time-lapse imaging of the disruption of tRFFP-B16 cells with tRFFP disappearance within the first hour of tRFFP-B16 inoculation in the non-immunized mice. The time-lapse intravital imaging was acquired by air 20×/0.75 NA objective. tRFFP-B16 cells are shown in magenta. Scale bar, 30 μm.

Movie S5: *In vivo* time-lapse imaging of the livers in non-immunized mice injected with a mixture of a 1:1 ratio of MLS-HyPer7-B16 cells and tRFFP-C3-B16 cells via the spleen. The top row shows fluorescence images, the middle row shows the HyPer7 ratio (F488/F405) images of MLS-HyPer7-B16 cells, and the bottom row shows the C3 ratio (FRET/CFP) images of tRFFP-C3-B16 cells. Time-lapse intravital imaging was acquired by air 20×/0.75 NA objective. Rosa-mTom cells are shown in blue, tRFFP-C3-B16 tumor cells are shown in magenta, and MLS-HyPer7-B16 cells are shown in green. Scale bar, 20 μm.

Movie S6: *In vivo* time-lapse imaging of the livers in non-immunized mice injected with a

mixture of a 1:1 ratio of MLS-HyPer7-B16 cells and tfRFP-C3-B16 cells via the spleen after injection of NAC. The top row shows fluorescence images, the middle row shows the HyPer7 ratio (F488/F405) images of MLS-HyPer7-B16 cells, and the bottom row shows the C3 ratio (FRET/CFP) images of tfRFP-C3-B16 cells. Time-lapse intravital imaging was acquired by air 20×/0.75 NA objective. Rosa-mTom cells are shown in blue, tfRFP-C3-B16 tumor cells are shown in magenta, and MLS-HyPer7-B16 cells are shown in green. Scale bar, 20 μm .

Movie S7: *In vivo* time-lapse imaging of the liver within one hour after injecting tfRFP-immunized mice with GSDME-GFP^{hi}tfRFP-B16 cells. GSDME-GFP is shown in green, and tfRFP is shown in magenta. Scale bar, 20 μm .